Front. Chem. China 2007, 2(1): 21–26
DOI 10.1007/s11458-007-0005-9

RESEARCH ARTICLE

LIU Chunyan, JIN Zhaoguo, ZHANG Wengong

Nanocarbon-poly(methyl methacrylate) composite materials

Abstract Nanocarbon–poly(methyl methacrylate) sols were prepared by pulsed laser ablation at the interface of target submerged in flowing liquid (PLA-IT/SFL) method, and the corresponding composite films were prepared by solution-casting. Spectra results indicated that there existed interactions between nanocarbon and the polymethyl methacrylate (PMMA) matrix, which was consistent with the decrease in glass transition temperature of the composites with increase of carbon content. TEM images revealed that a carbon encapsulated core/shell structure was formed in the composites, which could ensure good dispersion of carbon nanoparticles within the PMMA matrix. The decomposition of the composites was less influenced by the introduction of nanocarbon particles.

Keywords pulsed laser ablation, nanocarbon, poly(methyl methacrylate), composite materials

1 Introduction

In recent years there has been increasing interest involving the preparation of nanomaterials by pulsed laser ablation. Ogale et al. [1,2] first prepared metastable materials by pulsed laser ablation at the liquid–solid interface. Yang et al. [3−6] obtained diamond nano-crystals with cubic and hexagonal structures by pulsed laser induced liquid–solid (acetone and water–graphite) interfacial reaction at room temperature and pressure, and carbonitride nano-crystals with different structures by pulsed laser ablation on the graphite target immersed in hartshorn [7−10]. Zheng et al. [11−14] also prepared diamond nano-crystals and carbon nanotubes. Zhang et al. suggested and developed a novel method for preparation of nano sol by pulsed laser ablation at the rotative solid target submerged in the flowing liquid, which can also successively obtain many kinds of organic, inorganic nano-sols, and importantly, nanofabrication of solid target, chemical reaction and surface modification of nanoparticles can be carried out at the same time. We have obtained many kinds of metals [15,16], metal alloys [17], metal-oxides [18,19] and other organic, inorganic nano sols by this method. Recently, nanocarbon/polymer composite materials have attracted more and more interests [20–23], including poly (methyl methacrylate)/graphite slice nano conductive composite materials, polyethylene/carbon black conductive composite materials, graphite/polystyrene nano composite materials *etc*. We prepared *in-situ* nanocarbon and nanocarbon/polystyrene composite materials by the pulsed laser ablation method [24], in which the nanocarbon was well dispersed. For these materials the glass transition temperature fell distinctly, and the tenacity and thermal stability increased by introduction of a little nanocarbon. This work is mainly focused on the preparation of nanocarbon/poly (methyl methacrylate) composite materials, and their structure and properties are also investigated.

Translated from *Acta Polymerica Sinica* 2006, 2(2) (in Chinese)

LIU Chunyan, JIN Zhaoguo, ZHANG Wengong (✉)
Institute of Polymer Science, College of Chemistry & Materials Science, Fujian Normal University, Fuzhou 350007, China
E-mail: wgzhang@fjnu.edu.cn

2 Experimental

2.1 Materials

Acetic ether: analytically pure, purchased from the Shanghai Shiyi Chemical Reagent Co., Ltd., redistilled twice under reducing pressure prior to use. Poly (methyl methacrylate) (PMMA): industrial grade, purchased from the Beijing Yanshan Petrochemical Co., Ltd. Graphite powder: spectroscopic pure, supplied by Tianjin Kermel Chemical Reagent Co., Ltd., pressed into a round target with a diameter of 13 mm and a thickness of 2–3 mm. Flowing liquid: acetic ether solutions of PMMA with the concentration of 10‰ (sample 1), 5‰ (sample 2), 3‰ (sample 3), 2‰ (sample 4) and 1‰ (sample 5), respectively.

2.2 Instruments

The pulsed laser beams were produced from a DCR-3G (Nd: YAG) solid laser generator, produced by Spectra Physics Inc. in the U.S., with a wavelength of 532 nm, pulsed width of 8 ns and repeated frequency of 10 Hz. The device for the continuous synthesizing of the nano sol by pulsed laser ablation (Fig. 1) was assembled for this study by the authors [25].

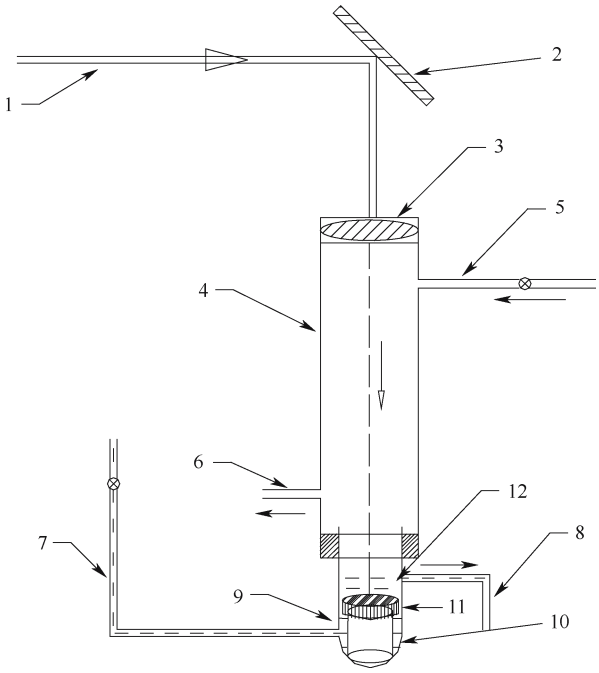

1. Puled laser beam 2. Reflector 3. Focusing lens 4. Quartz tube
5. Nitrogen gas entrance 6. Nitrogen gas exit 7. Flowing liquid entrance
8. Nano sol entrance 9. Reaction container 10. Bracket
11. Solid target 12. Nano sol

Fig. 1 Device for pulsed laser continuous ablation for synthesis of nano sols

2.3 Preparation of nanocarbon/poly(methyl methacrylate) (C-PMMA) sol and composite materials

Acetic ether solution of PMMA with a velocity of about 1 d/s controlled through a flowmeter was flowing over the surface of the graphite target placed in the quartz tube of the synthesis device, the depth of the flowing liquid over the surface of the solid target was approximately 1–2 mm. Pulsed laser beams with wavelength of 532 nm was focused at the liquid–solid interface, the diameter of laser focus spot was less than 1.0 mm, and the power density in the laser focus spot was as high as 10^8 W/cm^2, so a micro-area with high temperature, high pressure and high density in the laser focus spot was produced, and the graphite target and acetic ether solution in the micro-area were instantly gasified, ionized, decomposed and became a plasma mass, which rapidly quenched and condensed in the special sharply cooling surroundings during an instant of 8 ns. Consequently, the nanocarbon particles with a great deal of dangling bonds on their surface were produced, which can be well dispersed in the liquid at the same time. Pure nitrogen was passing through the synthesis device in the whole preparation process.

The C-PMMA sol was cast on a smooth glass slide, so the corresponding composite films were obtained after volatilizing the acetic ether by infrared light.

2.4 Characterizations

A JEOL transmission electron microscope TEM-1200EX was used for morphological observations. An FT–IR spectrometer AVATAR360 from Thermo Nicolet Company, a UV–Vis spectrometer TU-1800PC from Beijing Puxi General Instrument Co. Ltd. and a fluorescence spectrometer F900 from Edinburgh Analytical Instrument Company were used for the spectroscopic analyses. Dynamic mechanical measurements were performed with a DMTA-4 instrument of Rheometric Scientific Inc. at a frequency of 1.0 Hz and a heating rate of 2.0 K/min. Differential scanning calorimetry was performed in a Perkin-Elmer DSC-7 instrument. Samples were heated at a scanning rate of 10 K/min under nitrogen purge of 50 mL/min. Thermogravimetric analysis was carried out with a Shimadzu DT-40 instrument in nitrogen atmosphere, and the heating rate was 10 K/min.

3 Results and discussion

3.1 FT–IR, UV–Vis and fluorescence spectroscopy analyses

The mass difference of the graphite target before and after ablation by pulsed laser is the mass of the nanocarbon in the C-PMMA sol, and the mass ratio of nanocarbon and PMMA in the sol is the nanocarbon content in the composite film, the results are shown in Table 1.

Table 1 Mass content of nanocarbon in C-PMMA composites

Samples	0	1	2	3	4	5
Nano-carbon content (wt%)	0.000	0.345	0.525	1.025	1.398	2.320

The FT–IR spectra for the representative film samples 0, 1, 3, 5, raw graphite and the as-prepared nanocarbon are shown in Fig. 2. From it we can see that, the as-prepared nanocarbons by this method, compared to raw graphite, exhibit some additional absorption peaks. For example, the antisymmetry stretching vibration absorption peak of the $–CH_3$ group ($\upsilon_{C–H}$) at 2959 cm^{-1}, the antisymmetry stretching vibration absorption peak of the $–CH_2–$ group ($\upsilon_{C–H}$) at 2925 cm^{-1}, the mutual symmetry stretching vibration absorption peak of the $–CH_3$ and $–CH_2–$ groups ($\upsilon_{C–H}$) at 2858 cm^{-1}, the stretching vibration absorption peak of the C=O group at 1727 cm^{-1}, the symmetry transform vibration absorption peak of the C=O group at 1381 cm^{-1}, and the stretching vibration absorption peak of the C–O–C group at 1274 cm^{-1}. This phenomenon is supposed to be the results of the decomposition of acetic ether during pulsed laser ablation and the adsorption of its group fragments on the surface of the nanocarbon particles. Because of the surface modification of nanocarbon by a lot of group fragments during the preparation, the nanocarbon particles could be well dispersed within the PMMA matrix. Moreover, compared to blank sample 0, the samples 1, 3, and 5 all exhibited two stretching vibration absorption peaks assigned to nanocarbon at 1629 cm^{-1} and 1063 cm^{-1}, and the relative intensity of the two peaks increased gradually from sample 1 to sample 5. So the hydrogen bond and the

strong Van der Waals' effect between the polar side groups of PMMA molecules and the hydrogen and oxygen groups, adsorbed on the surface of nanocarbon particles, had a certain effect on as-obtained nano C-PMMA composite materials in morphology, optical and mechanical properties.

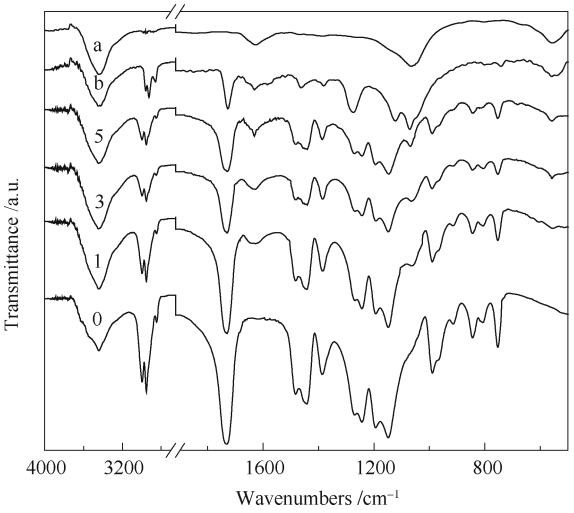

Fig. 2 FT–IR spectra for the film samples 0, 1, 3, 5, raw graphite (a) and the as-prepared nanocarbon (b)

The UV–Vis spectra of the representative sol samples 0, 1, 3, 5 are shown in Fig. 3. A single big absorption peak at 258.0 nm was observed for sample 0. In addition to the big adsorption peak at 258.0 nm a side peak at 263.0 nm and two weak adsorption peaks at 275.0 nm and 295.0 nm, respectively, were detected for samples 1, 3, 5. In the UV–Vis curves of C-PMMA sol samples the maximal absorption peak at 258.0 nm was attributed to the π electrons transition in the C=O groups of PMMA, while the side peak at 263.0 nm was assigned to the excited transition of the valence electrons on nanocarbon particle surface, and the two weak peaks at 275.0 nm and 295.0 nm were thought to be exciton absorption ones of nanocarbon. The low absorption of all samples in the range of 350–800 nm indicates that the obtained C-PMMA composite films are almost transparent in the visual region.

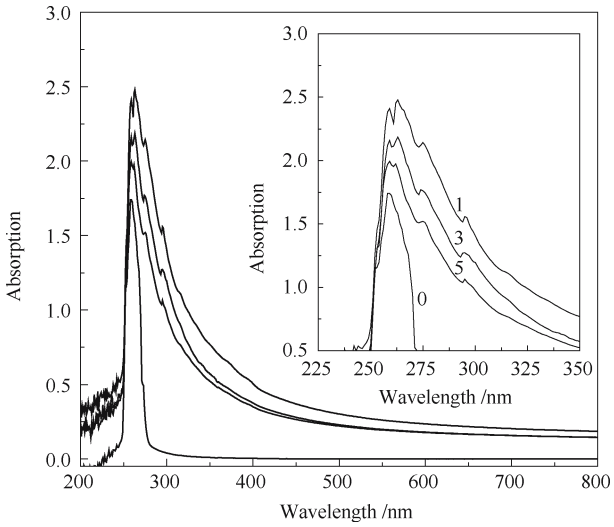

Fig. 3 UV–Vis spectra for the sol samples 0, 1, 3 and 5

Figure 4 shows the fluorescence spectra of the representative film samples 0, 1, 3 and 5. A wide excitation peak at 284.00 nm was observed for sample 0, while an excitation peak at 286.0 nm was shown for samples 1, 3, 5. Not only did the excitation peaks of samples 1, 3, 5 show a red shift, but also the intensity decreased with the increase of the nanocarbon content from sample 0 to sample 5. There was a strong emission peak at 330.0 nm for sample 0, while two broad emission peaks at 334.0 nm and 375.0 nm were observed for

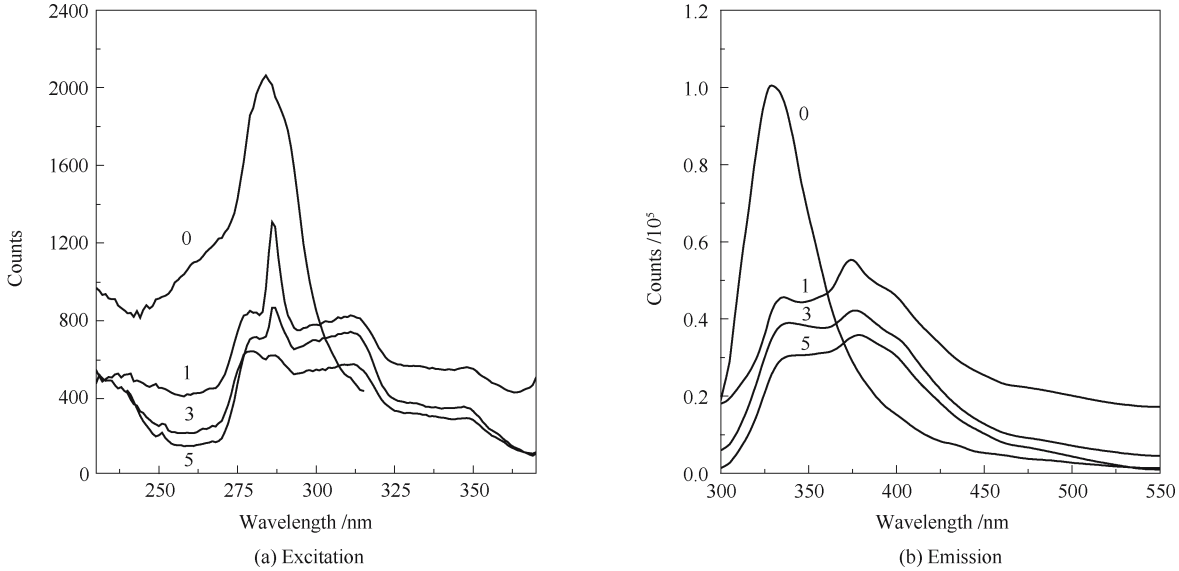

Fig. 4 Fluorescence spectra for the film samples 0, 1, 3 and 5

samples 1, 3, 5. Similar to the excitation peaks, the emission peaks of samples 1, 3, 5 showed a red shift, and the intensity decreased with the increase of the nanocarbon content from sample 0 to sample 5. It is deduced that the strong excitation peak results from π electrons transition of ester groups in PMMA macromolecules. With the addition of nanocarbon particles, on the one hand, because of the hydrogen bonding and strong Van der Waals' effect between the polar side groups of PMMA macromolecules and the adsorbed carbon, hydrogen and oxygen polar groups on the surface of nanocarbon particles, the π electrons may easily transfer to the surface of nanocarbon particles. As a result the quantity of excited electrons in PMMA is reduced, and the intensities of the maximal excitation peaks decrease markedly with the increasing content of nanocarbon particles. On the other hand, the π electron fluidity is enhanced because of the electron transfer between the polar side groups in PMMA macromolecules and the adsorbed polar groups on the surface of nanocarbon particles, the π electron transition becomes easy by excitation, and the excitation and emission peaks show red shifts.

3.2 TEM analysis

Figure 5 shows the morphology of the sol samples 1, 3 and 5. The nanocarbon particles in samples 1 and 3 exhibit a spherical shape with size of 30–50 nm and are well dispersed in the PMMA matrix while the nanocarbon particles in sample 5 display a clear carbon encapsulated core/shell structure, and the size of cores is still in the range of 30–50 nm. Presumably, the nanocarbon particles, prepared by this method, adsorbing *in situ* a lot of organic group fragments on their surface from decomposed acetic ether molecules during preparation, exhibit strong interaction with PMMA macromolecules. When these macromolecules are adsorbed onto the surface of the nanocarbon particles, the displayed core/shell structures are formed. This is consistent with the trend of the shift of characteristic spectrum peaks with the change of nanocarbon particle content in the composites.

3.3 DMTA, DSC and TGA analysis

Figure 6 represents the temperature dependence of tanδ from DMTA measurements for film samples 0, 1, 3, and 5. The

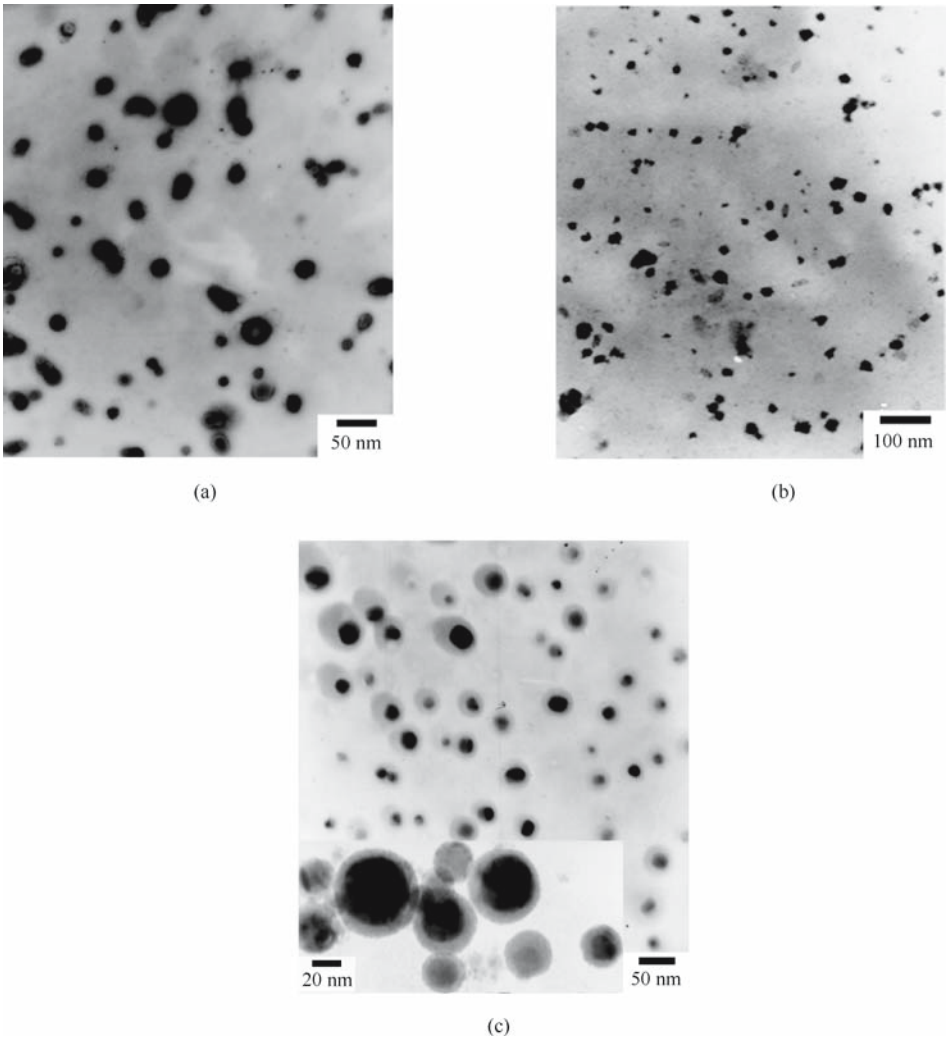

Fig. 5 TEM images for the sol samples. (a) sample 1; (b) sample 3; (c) sample 5

glass transition temperature (T_g) of sample 0 with no nanocarbon particles is 105.1°C, while the T_g of the other 3 samples with increasing content of nanocarbon particles are 99.8°C, 88.5°C, 75.8°C, respectively. The DSC thermograms of the same film samples are shown in Fig. 7. From it we can see that, the glass transition temperature of the film samples 0, 1, 3 and 5 are 103.0°C, 97.2°C, 87.6°C, 76.7°C, respectively. They are consistent with the results from DMTA measurements. That is to say, the T_g of PMMA distinctly decreases with the introduction of nanocarbon. It is supposed presumably that, on the one hand, the nanocarbon particles are very small and contain a large number of polar groups on their surface, and they can disperse well within the PMMA matrix. Meanwhile, the strong interaction between the polar side groups in PMMA macromolecules and the adsorbed polar groups on the surface of nanocarbon particles may weaken the interactions among PMMA macromolecules. On the other hand, the introduced nanocarbon particles may increase the free volume of the composites, so there will be more interspace for the movement of PMMA macromolecules. The above two reasons lead to the evident reduction of activation energy for the movement of PMMA chain segments and the distinct decrease of glass transition temperature.

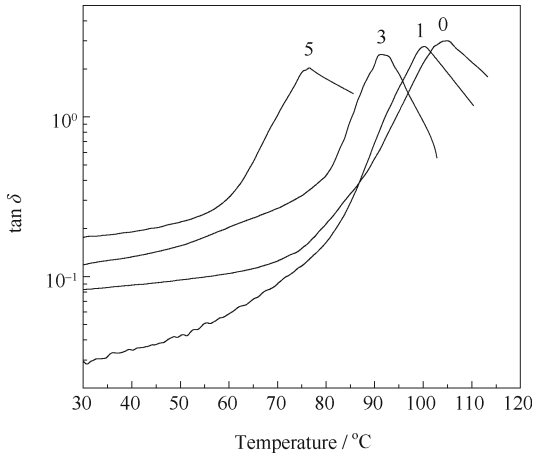

Fig. 6 Temperature dependence of tanδ for the film samples 0, 1, 3 and 5

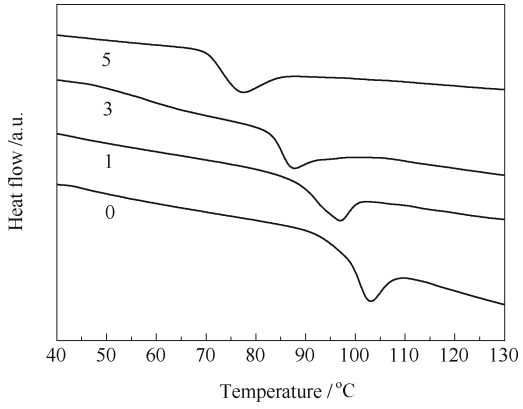

Fig. 7 DSC curves for the film samples 0, 1, 3 and 5

Figure 8 indicates the TGA results of the film samples 0, 1, 3 and 5. All samples displayed evident weight loss at 250–440°C, but the introduction and content of nanocarbon particles had little impact on the temperature dependence and the value of weight loss. It implies that nanocarbon particles have no distinct influence on PMMA in thermal decomposability.

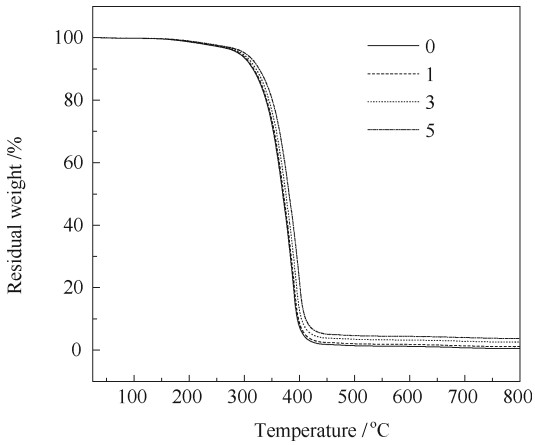

Fig. 8 TGA curves for the film samples 0, 1, 3 and 5

In conclusion, the C-PMMA sols in acetic ether were prepared by PLA-IT/SFL method, and the corresponding C-PMMA composite films were also obtained. Spectra results indicated that there existed some interactions between nanocarbon particles and the PMMA matrix. The introduced nanocarbon resulted in a decrease in the glass transition temperature of the PMMA. TEM images revealed that a carbon-encapsulated core/shell structure could be formed in the C-PMMA composites. The thermal decomposability of the composites was less influenced by the introduction of nanocarbons.

Acknowledgements This work was supported by the National Natural Science Foundation of China (Grant No. 50272014) and the Fujian Provincial Natural Science Foundation of China (Grant No. 2001F005).

References

1. Ogale S B, Patil P P, Phase D M, Bhandarkar Y V, Kulkarni S K, Ghaisas S V, Kanetkar S M. Synthesis of metastable phases via pulsed-laser-induced reactive quenching at liquid-solid interfaces. Phys Rev B, 1987, 36(16): 8237−8250
2. Ogale S B, Roorda S, Saris F W, Polman A, Quentin F O P. Pulsed laser oxidization and nitridation of metal surface immersed in liquid media. Appl Phys Lett, 1987, 50(3): 138−140
3. Wang J B, Liu Q X, Yang G W, Hu G B, You J Q. Nano-crystalline diamond preparation by inducing reaction at liquid-solid interface. Chinese Journal of Materials Research, 1998, 12(3): 323−325 (in Chinese)
4. Wang J B, Liu Q X, Yang G W, Chen X Q, You J Q. Nano-crystalline diamond prepared by laser ablation solid target in liquid. Chinese Journal of High Pressure Physics, 1998, 12(4): 303−306 (in Chinese)

5. Yang G W, Wang J B, Liu Q X. Preparation of nano-crystalline diamonds using pulsed laser induced reactive quenching. Journal of Physics: Condensed Matter, 1998, 10(35): 7923−7927
6. Wang J B, Yang G W. Cubic and hexagonal structures of diamond nanocrystals formed upon pulsed laser induced liquid–solid interfacial reaction. Chemical Physics Letters, 2002, 361(1-2): 86−90
7. Wang J B, Liu Q X, Yang G W. The preparation of cubic C_3N_4 by pulsed-laser inducing reaction in liquid-solid interface. Chemical Journal of Chinese Universities, 1998, 19(11): 1719−1720 (in Chinese)
8. Liu Q X, Wang J B, Yang G W. Nano-crystalline carbon nitrides prepared by laser ablating solid target in liquid. Microfabrication Technology, 1998, (2): 24−30 (in Chinese)
9. Wang J B, Ren Z A, Yang G W. Preparation of Carbon Nitride Nano-crystals with β-and a-phases Using Pulsed-Laser Induced Liquid-Solid interfacial Reaction. Natural Science Journal of Xiangtan University, 2000, 22(4): 122−125 (in Chinese)
10. Yang G W, Wang J B. Carbon nitride nanocrystals having cubic structure using pulsed laser induced liquid-solid interfacial reaction. Applied Physics A: Materials Science & Processing, 2000, 71(3): 343−344
11. Wang Y H, Yu R Q, Liu C Y, Huang R B, Zheng L S, Zhang X F, Hu G, Zhang Z. Production of diamond nano-spherulite at carbon water interface by laser ablation and its characterization by TEM. Chemical Journal of Chinese Universities, 1997, 18(1): 124−126 (in Chinese)
12. Wang Y H, Huang Q J, Chen Z, Huang R B, Zheng L S. Diamond nanospherulite: A novel material produced at carbon-water interface by pulsed laser ablation. Science in China series B, 1997, 27(6): 496−502 (in Chinese)
13. Cheng D D, Yu R Q, Liu C Y, Zhang Q, Wang Y H, Huang R B, Zhan M G, Zheng L S. Preparation of carbon nanotubes from laser ablation. Chemical Journal of Chinese Universities, 1995, 16(6): 948−949 (in Chinese)
14. Wang Y H, Zhang Q, Liu C Y, Huang R B, Zheng L S. Production of carbon nanotubes at carbon/water interface by pulsed-laser ablation. Acta Physico-Chimica Sinica, 1996, 12(10): 905−909 (in Chinese)
15. Zhang Y, Chen W Z, Zhang W G.. Preparation and disperse stability of nano-iron/ethanol sol prepared by pulsed laser ablation. Acta Chimica Sinica, 2003, 61(1): 141−145 (in Chinese)
16. Zhang Y, Chen W Z, Zhang W G. Study on nano-cobalt/ethanol sol prepared by pulsed laser ablation. Chemical Journal of Chinese Universities, 2003, 24(2): 337−339 (in Chinese)
17. Zhang W G, Jin Z G. Research on successive preparation of nano-FeNi alloy and its ethanol sol by pulsed laser ablation. Science in China series B, 2004, 47(2): 159−165
18. Zhang W G, Zhang Y, Wang L H, Ling Q D, Tang J Y. Study on the preparation of novel nano-rare earth oxides/organic polymer hybrid films and their optical properties. In: International Conference on Materials for Advanced Technologies, Singapore, 2001, 232
19. Zhang W G, Zhang Y, Tang J Y, Wang L, Ling Q D. Study on preparation and optic properties of nano europium oxide-ethanol sol by pulsed laser ablation. Thin Solid Films, 2002, 417: 43−46
20. Quan C Z, Shen J W, Chen X M. Preparation and properties of polypropylene/graphite electrically conductive nanocomposites. Acta Polymerica Sinica, 2003, (6): 831−836 (in Chinese)
21. Chen G H, Wu C L, Wu D J, Weng W G, Huang S X, Lin S X. Investigation on the PMMA/graphite platelet nanocomposites and their conduction properties. Acta Polymerica Sinica, 2003, (5): 742−745 (in Chinese)
22. Shen L, Yi X S. The morphology of PE/CB conductive composites, Acta Polymerica Sinica, 2001, (1): 130−133 (in Chinese)
23. Chen G H, Weng W G, Wu D J, Wu D C, Chen J G, Ye L H, Yan W L. Investigation on the nano dispersion of graphite into polymer matrix. Acta Polymerica Sinica, 2001, (6): 803−806 (in Chinese)
24. Jin Z G, Zhang W G. Research on nanocarbon-polystyrene hybrid materials prepared in situ by pulsed laser ablation. China Plastics, 2004, 18(6): 48−53 (in Chinese)
25. Zhang W G, Zhang Y. CN Patent, B22F9/04, 02255143.3. 2003-08-27 (in Chinese)